Electronic Supplementary Material (ESI) for Journal of Materials Chemistry A.


# Towards higher electrochemical stability of electrolytes: lithium salt design through *in silico* screening

*Dale A. Osborne,[a] Michael Breedon,[b] Thomas Rüther,[c] and Michelle J.S. Spencer [*,a,d]*

*a) School of Science, RMIT University, GPO Box 2476, Melbourne, Victoria 3001, Australia.*
*b) CSIRO Manufacturing, Private Bag 10, Clayton South, Victoria 3169, Australia.*
*c) CSIRO Energy, Private Bag 10, Clayton South, Victoria 3169, Australia*
*d) ARC Centre of Excellence in Future Low-Energy Electronics Technologies, School of Science, RMIT University, Melbourne, Victoria 3001, Australia*

## Electronic Supplementary Information

**Table S1** – List of abbreviations for anion structures investigated in this study.

| Abbreviation | | Chemical Name |
|---|---|---|
| $R_1$ | TFSI | bis((trifluoromethyl)sulfonyl)imide |
| $R_2$ | FSI | bis(fluorosulfonyl)imide |
| $R_3$ | FTFSI | (fluorosulfonyl)((trifluoromethyl)sulfonyl)imide |
| $S_1$ | MSI | bis(methylsulfonyl)imide |
| $S_2$ | ESI | bis(ethylsulfonyl)imide |
| $S_3$ | BETI | bis((perfluoroethyl)sulfonyl)imide |
| $S_4$ | TFESI | bis((2,2,2-trifluoroethyl)sulfonyl)imide |
| $S_5$ | TbSI | bis(tert-butylsulfonyl)imide |
| $S_6$ | NFSI | bis((1,1,1,3,3,3-hexafluoro-2-(trifluoromethyl)propan-2-yl)sulfonyl)imide |
| $S_7$ | CSI | bis(cyanosulfonyl)imide |
| $S_8$ | CmSI | bis(cyanomethyl)sulfonyl)imide |
| $S_9$ | MOSI | bis(methoxysulfonyl)imide |
| $A_1$ | HMSI | (hydrosulfonyl)(methylsulfonyl)imide |
| $A_2$ | FMSI | (fluorosulfonyl)(methylsulfonyl)imide |
| $A_3$ | HESI | (ethylsulfonyl)(hydrosulfonyl)imide |
| $A_4$ | MESI | (ethylsulfonyl)(methylsulfonyl)imide |
| $A_5$ | FPFESI | (fluorosulfonyl)((perfluoroethyl)sulfonyl)imide |
| $A_6$ | MTbSI | (tert-butylsulfonyl)(methylsulfonyl)imide |
| $A_7$ | TFNFSI | ((1,1,1,3,3,3-hexafluoro-2-(trifluoromethyl)propan-2-yl)sulfonyl)((trifluoromethyl)sulfonyl)imide |
| $A_8$ | FCSI | (cyanosulfonyl)(fluorosulfonyl)imide |
| $A_9$ | TFCSI | (cyanosulfonyl)((trifluoromethyl)sulfonyl)imide |

**Table S2** – Anion natural charge for each atom of the sulfonyl core, and sum of the charges for each functional group, calculated from the M06-2X/6-311$^{++}$G(2d,p) geometry.

| | | N | $S_1$ | $S_2$ | $O_1$ | $O_2$ | $O_3$ | $O_4$ | R’ | R’’ |
|---|---|---|---|---|---|---|---|---|---|---|
| | | | | | | (*e*) | | | | |
| $R_1$ | LiTFSI | -1.26 | 2.27 | 2.27 | -0.97 | -0.97 | -0.96 | -0.96 | -0.22 | -0.22 |
| $R_2$ | LiFSI | -1.23 | 2.56 | 2.56 | -0.96 | -0.96 | -0.95 | -0.95 | -0.53 | -0.53 |
| $R_3$ | LiFTFSI | -1.24 | 2.27 | 2.56 | -0.96 | -0.97 | -0.95 | -0.96 | -0.53 | -0.22 |
| $S_1$ | LiMSI | -1.26 | 2.32 | 2.32 | -1.03 | -1.03 | -1.01 | -1.01 | -0.15 | -0.15 |
| $S_2$ | LiESI | -1.26 | 2.33 | 2.33 | -1.01 | -1.01 | -1.03 | -1.04 | -0.15 | -0.15 |
| $S_3$ | LiBETI | -1.25 | 2.30 | 2.30 | -0.96 | -0.96 | -0.96 | -0.96 | -0.26 | -0.26 |
| $S_4$ | LiTFESI | -1.26 | 2.34 | 2.34 | -0.98 | -0.98 | -1.01 | -1.01 | -0.22 | -0.22 |
| $S_5$ | LiTbSI | -1.30 | 2.35 | 2.35 | -1.01 | -1.01 | -1.02 | -1.02 | -0.17 | -0.17 |
| $S_6$ | LiNFSI | -1.28 | 2.40 | 2.40 | -0.96 | -0.96 | -0.94 | -0.94 | -0.36 | -0.36 |
| $S_7$ | LiCSI | -1.22 | 2.33 | 2.33 | -0.94 | -0.94 | -0.94 | -0.94 | -0.34 | -0.34 |
| $S_8$ | LiCmSI | -1.25 | 2.35 | 2.35 | -0.98 | -0.98 | -1.01 | -1.01 | -0.24 | -0.24 |
| $S_9$ | LiMOSI | -1.27 | 2.54 | 2.55 | -0.98 | -0.99 | -0.99 | -0.98 | -0.44 | -0.44 |
| $A_1$ | LiHMSI | -1.26 | 2.32 | 2.19 | -1.01 | -1.00 | -1.03 | -1.02 | -0.04 | -0.15 |
| $A_2$ | LiFMSI | -1.25 | 2.55 | 2.32 | -0.99 | -1.00 | -0.97 | -1.00 | -0.53 | -0.14 |
| $A_3$ | LiHESI | -1.26 | 2.19 | 2.32 | -1.00 | -1.03 | -1.02 | -1.01 | -0.04 | -0.15 |
| $A_4$ | LiMESI | -1.26 | 2.33 | 2.32 | -1.01 | -1.01 | -1.03 | -1.03 | -0.15 | -0.15 |
| $A_5$ | LiFPFESI | -1.24 | 2.56 | 2.30 | -0.95 | -0.96 | -0.95 | -0.96 | -0.53 | -0.26 |
| $A_6$ | LiMTbSI | -1.28 | 2.34 | 2.33 | -1.01 | -1.03 | -1.02 | -1.02 | -0.15 | -0.17 |
| $A_7$ | LiTFNFSI | -1.27 | 2.39 | 2.28 | -0.95 | -0.95 | -0.96 | -0.96 | -0.21 | -0.38 |
| $A_8$ | LiFCSI | -1.22 | 2.33 | 2.56 | -0.95 | -0.95 | -0.95 | -0.94 | -0.53 | -0.35 |
| $A_9$ | LiTFCSI | -1.23 | 2.33 | 2.26 | -0.96 | -0.95 | -0.96 | -0.94 | -0.20 | -0.35 |

**Table S3** – Lithium salt natural charge for each atom of the sulfonyl core, and sum of the charges for each functional group, calculated from the M06-2X/6-311$^{++}$G(2d,p) geometry.

| | | N | $S_1$ | $S_2$ | $O_1$ | $O_2$ | $O_3$ | $O_4$ | Li | R’ | R’’ |
|---|---|---|---|---|---|---|---|---|---|---|---|
| | | | | | | (*e*) | | | | | |
| $R_1$ | LiTFSI | -1.24 | 2.28 | 2.28 | -0.90 | -0.90 | -1.09 | -1.09 | 0.95 | -0.14 | -0.14 |
| $R_2$ | LiFSI | -1.21 | 2.59 | 2.59 | -0.89 | -0.89 | -1.08 | -1.08 | 0.96 | -0.50 | -0.50 |
| $R_3$ | LiFTFSI | -1.22 | 2.27 | 2.59 | -0.89 | -0.90 | -1.08 | -1.10 | 0.95 | -0.49 | -0.14 |
| $S_1$ | LiMSI | -1.25 | 2.33 | 2.30 | -0.95 | -0.98 | -1.13 | -1.12 | 0.95 | -0.08 | -0.07 |
| $S_2$ | LiESI | -1.25 | 2.33 | 2.30 | -0.95 | -0.99 | -1.13 | -1.12 | 0.95 | -0.08 | -0.06 |
| $S_3$ | LiBETI | -1.21 | 2.30 | 2.30 | -0.89 | -0.90 | -1.08 | -1.08 | 0.94 | -0.19 | -0.17 |
| $S_4$ | LiTFESI | -1.22 | 2.34 | 2.34 | -0.93 | -0.93 | -1.09 | -1.09 | 0.91 | -0.17 | -0.17 |
| $S_5$ | LiTbSI | -1.28 | 2.34 | 2.36 | -0.98 | -0.97 | -1.13 | -1.14 | 0.95 | -0.07 | -0.08 |
| $S_6$ | LiNFSI | -1.26 | 2.41 | 2.41 | -0.90 | -0.90 | -1.09 | -1.08 | 0.95 | -0.26 | -0.27 |
| $S_7$ | LiCSI | -1.20 | 2.34 | 2.34 | -0.88 | -0.88 | -1.07 | -1.07 | 0.96 | -0.27 | -0.27 |
| $S_8$ | LiCmSI | -1.26 | 2.36 | 2.37 | -0.93 | -0.92 | -1.08 | -1.07 | 0.93 | -0.18 | -0.21 |
| $S_9$ | LiMOSI | -1.23 | 2.53 | 2.56 | -0.91 | -0.93 | -1.05 | -1.08 | 0.94 | -0.45 | -0.39 |
| $A_1$ | LiHMSI | -1.24 | 2.30 | 2.20 | -0.97 | -0.93 | -1.12 | -1.12 | 0.95 | 0.00 | -0.06 |
| $A_2$ | LiFMSI | -1.23 | 2.58 | 2.33 | -0.89 | -0.94 | -1.08 | -1.12 | 0.95 | -0.53 | -0.07 |
| $A_3$ | LiHESI | -1.24 | 2.20 | 2.30 | -0.93 | -0.98 | -1.12 | -1.12 | 0.95 | 0.00 | -0.06 |
| $A_4$ | LiMESI | -1.25 | 2.30 | 2.33 | -0.95 | -0.99 | -1.13 | -1.12 | 0.95 | -0.08 | -0.06 |
| $A_5$ | LiFPFESI | -1.20 | 2.59 | 2.29 | -0.88 | -0.89 | -1.07 | -1.08 | 0.94 | -0.50 | -0.19 |
| $A_6$ | LiMTbSI | -1.25 | 2.32 | 2.34 | -0.95 | -0.99 | -1.13 | -1.12 | 0.95 | -0.09 | -0.06 |
| $A_7$ | LiTFNFSI | -1.25 | 2.39 | 2.28 | -0.90 | -0.90 | -1.08 | -1.07 | 0.94 | -0.13 | -0.29 |
| $A_8$ | LiFCSI | -1.20 | 2.34 | 2.59 | -0.88 | -0.88 | -1.08 | -1.08 | 0.96 | -0.50 | -0.27 |
| $A_9$ | LiTFCSI | -1.22 | 2.34 | 2.27 | -0.89 | -0.88 | -1.09 | -1.08 | 0.95 | -0.13 | -0.28 |

**Table S4** – Change in net charges (Δq) between the most stable anion and Li salt structure.

| | | | N | $S_1$ | $S_2$ | $O_1$ | $O_2$ (*e*) | $O_3$ | $O_4$ | Li | R’ | R’’ |
|---|---|---|---|---|---|---|---|---|---|---|---|---|
| Ref. | $R_1$ | LiTFSI | 0.017 | 0.012 | 0.012 | 0.064 | 0.064 | -0.138 | -0.138 | -0.046 | 0.076 | 0.076 |
| | $R_2$ | LiFSI | 0.024 | 0.031 | 0.031 | 0.073 | 0.073 | -0.129 | -0.129 | -0.044 | 0.034 | 0.034 |
| | $R_3$ | LiFTFSI | 0.025 | 0.003 | 0.030 | 0.068 | 0.069 | -0.132 | -0.134 | -0.046 | 0.036 | 0.081 |
| Symmetrical | $S_1$ | LiMSI | 0.015 | 0.010 | -0.020 | 0.082 | 0.051 | -0.123 | -0.107 | -0.052 | 0.064 | 0.081 |
| | $S_2$ | LiESI | 0.016 | 0.008 | -0.021 | 0.059 | 0.028 | -0.102 | -0.089 | -0.053 | 0.068 | 0.086 |
| | $S_3$ | LiBETI | 0.039 | -0.006 | 0.000 | 0.067 | 0.058 | -0.122 | -0.126 | -0.062 | 0.070 | 0.083 |
| | $S_4$ | LiTFESI | 0.035 | -0.002 | -0.002 | 0.058 | 0.058 | -0.084 | -0.084 | -0.086 | 0.052 | 0.052 |
| | $S_5$ | LiTbSI | 0.026 | -0.013 | 0.007 | 0.028 | 0.046 | -0.111 | -0.118 | -0.052 | 0.100 | 0.086 |
| | $S_6$ | LiNFSI | 0.018 | 0.009 | 0.009 | 0.051 | 0.052 | -0.144 | -0.143 | -0.052 | 0.103 | 0.097 |
| | $S_7$ | LiCSI | 0.020 | 0.015 | 0.015 | 0.059 | 0.059 | -0.131 | -0.131 | -0.044 | 0.070 | 0.070 |
| | $S_8$ | LiCmSI | -0.009 | 0.017 | 0.021 | 0.048 | 0.054 | -0.077 | -0.061 | -0.072 | 0.054 | 0.026 |
| | $S_9$ | LiMOSI | 0.039 | -0.009 | 0.016 | 0.068 | 0.063 | -0.061 | -0.095 | -0.063 | -0.010 | 0.054 |
| Asymmetrical | $A_1$ | LiHMSI | 0.018 | -0.019 | 0.012 | 0.036 | 0.067 | -0.087 | -0.099 | -0.053 | 0.038 | 0.087 |
| | $A_2$ | LiFMSI | 0.019 | 0.023 | 0.009 | 0.094 | 0.059 | -0.113 | -0.121 | -0.047 | 0.008 | 0.068 |
| | $A_3$ | LiHESI | 0.020 | 0.012 | -0.021 | 0.066 | 0.055 | -0.100 | -0.110 | -0.054 | 0.037 | 0.095 |
| | $A_4$ | LiMESI | 0.017 | -0.022 | 0.009 | 0.060 | 0.028 | -0.103 | -0.088 | -0.053 | 0.063 | 0.089 |
| | $A_5$ | LiFPFESI | 0.038 | 0.025 | -0.005 | 0.071 | 0.072 | -0.124 | -0.117 | -0.061 | 0.030 | 0.071 |
| | $A_6$ | LiMTbSI | 0.024 | -0.023 | 0.004 | 0.060 | 0.041 | -0.117 | -0.106 | -0.053 | 0.062 | 0.107 |
| | $A_7$ | LiTFNFSI | 0.021 | 0.001 | -0.002 | 0.045 | 0.043 | -0.120 | -0.111 | -0.058 | 0.089 | 0.091 |
| | $A_8$ | LiFCSI | 0.020 | 0.011 | 0.031 | 0.071 | 0.065 | -0.126 | -0.135 | -0.045 | 0.030 | 0.078 |
| | $A_9$ | LiTFCSI | 0.019 | 0.012 | 0.009 | 0.064 | 0.061 | -0.130 | -0.136 | -0.045 | 0.074 | 0.073 |

**Equation S1** - Calculation of lithium metal theoretical capacity.

$$Q = \frac{\left(1e \times 96{,}485.3321\ C.mol^{-1}\right)}{6.94\ g.mol^{-1} \times 3.6\ C.mAh^{-1}} = 3{,}861.87\ \approx 3{,}860\ mAh.g^{-1}$$

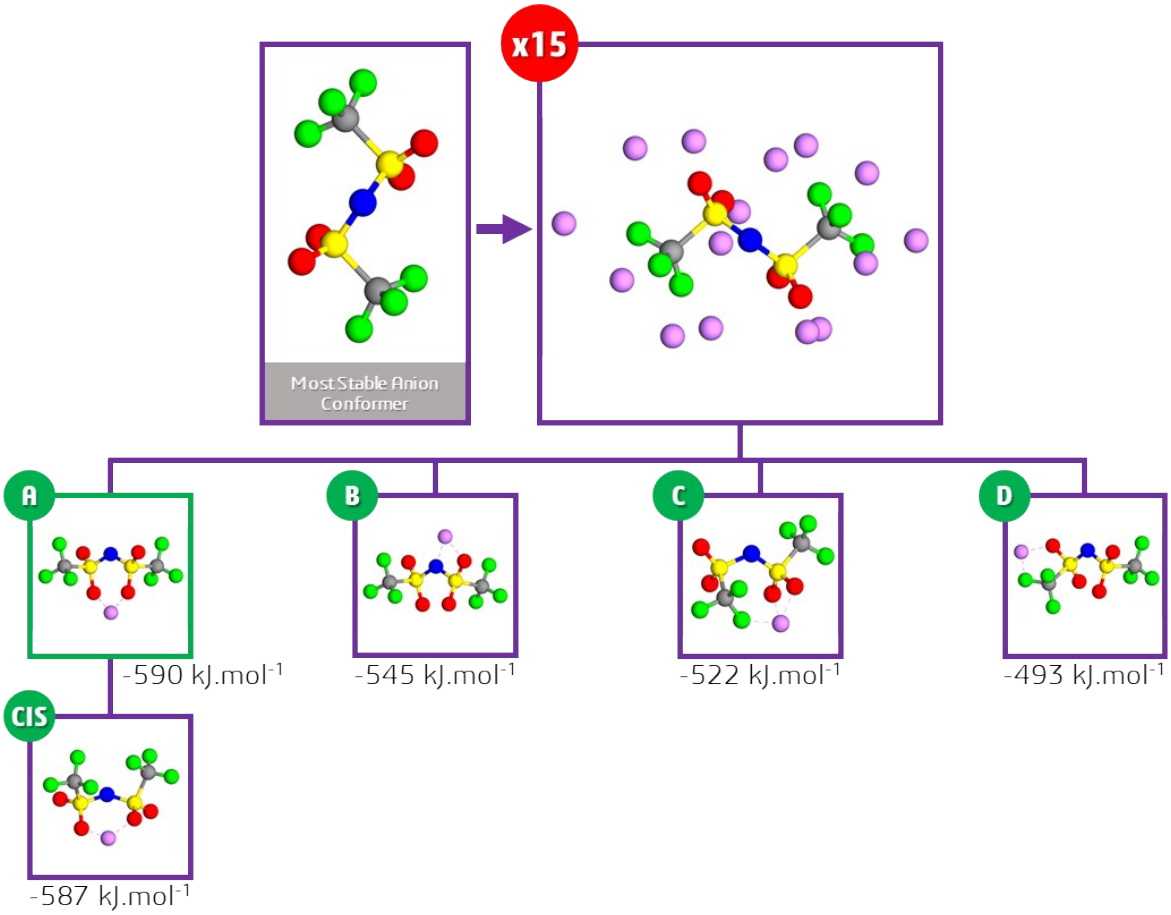


**Figure S1** – Conformer scan and lithiation site screening of $R_1$ ($TFSI^-$), depicting the 5 calculated unique adsorption sites and binding energies. The most stable site is outlined in green.

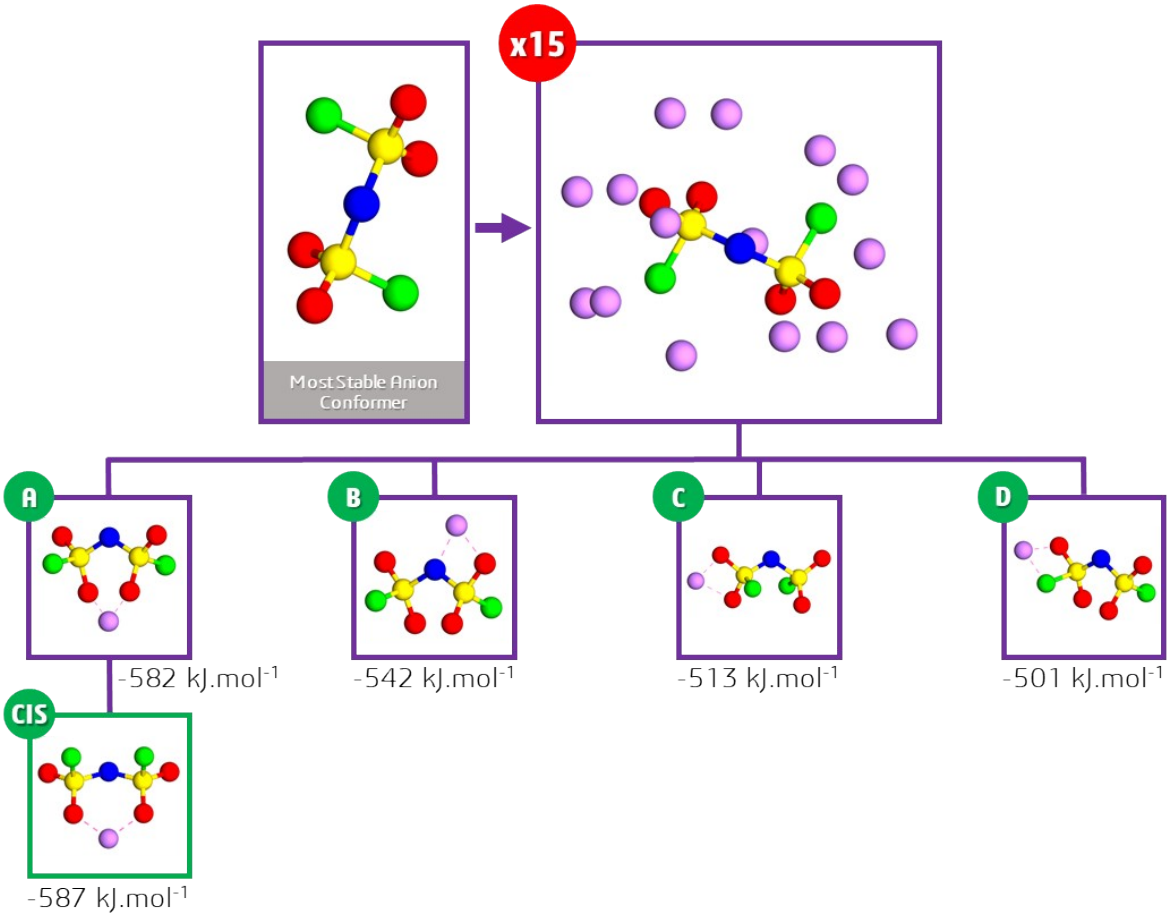


**Figure S2** – Conformer scan and lithiation site screening of $R_2$ ($FSI^-$), depicting the 5 calculated unique adsorption sites and binding energies. The most stable site is highlighted in green.

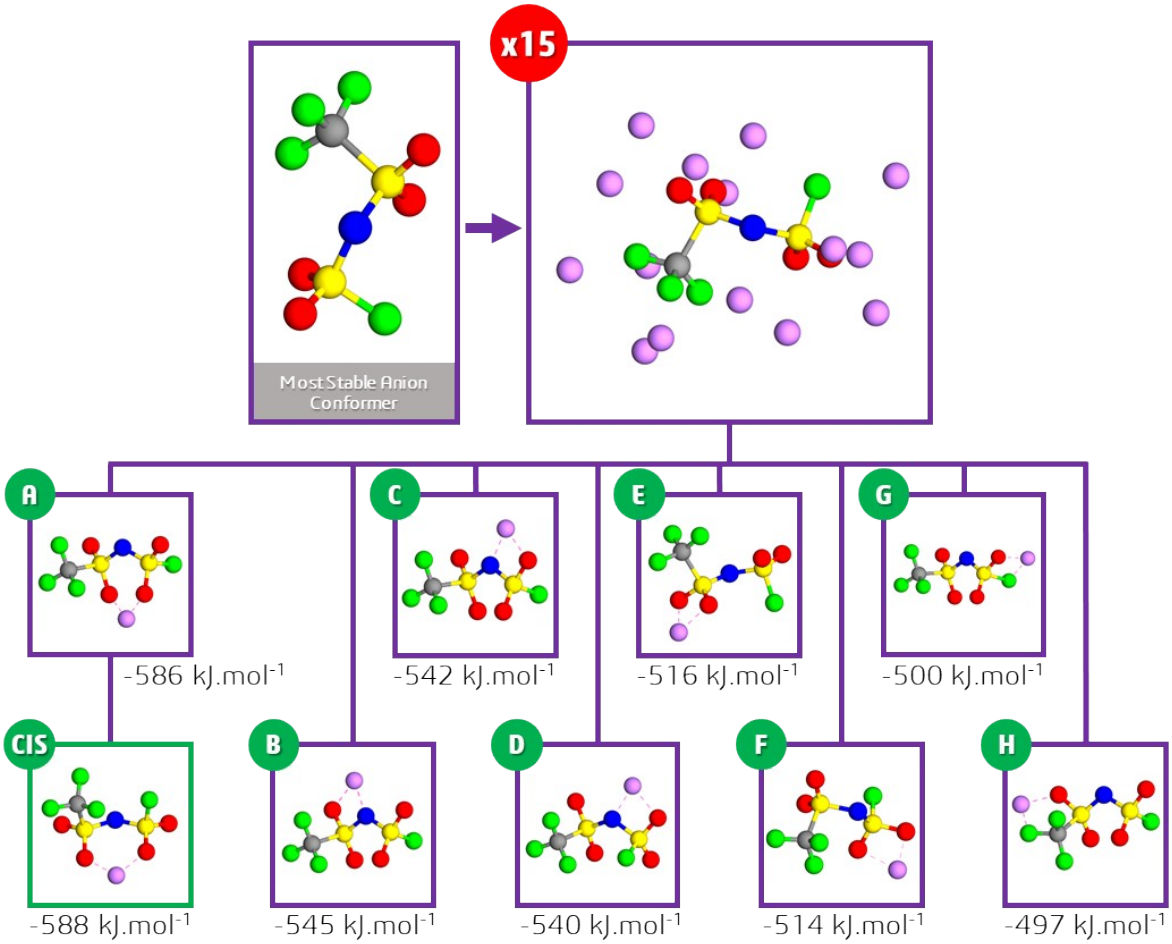


**Figure S3** – Conformer scan and lithiation site screening of $R_3$ ($FTFSI^-$), depicting the 9 calculated unique adsorption sites and binding energies. The most stable site is outlined in green.

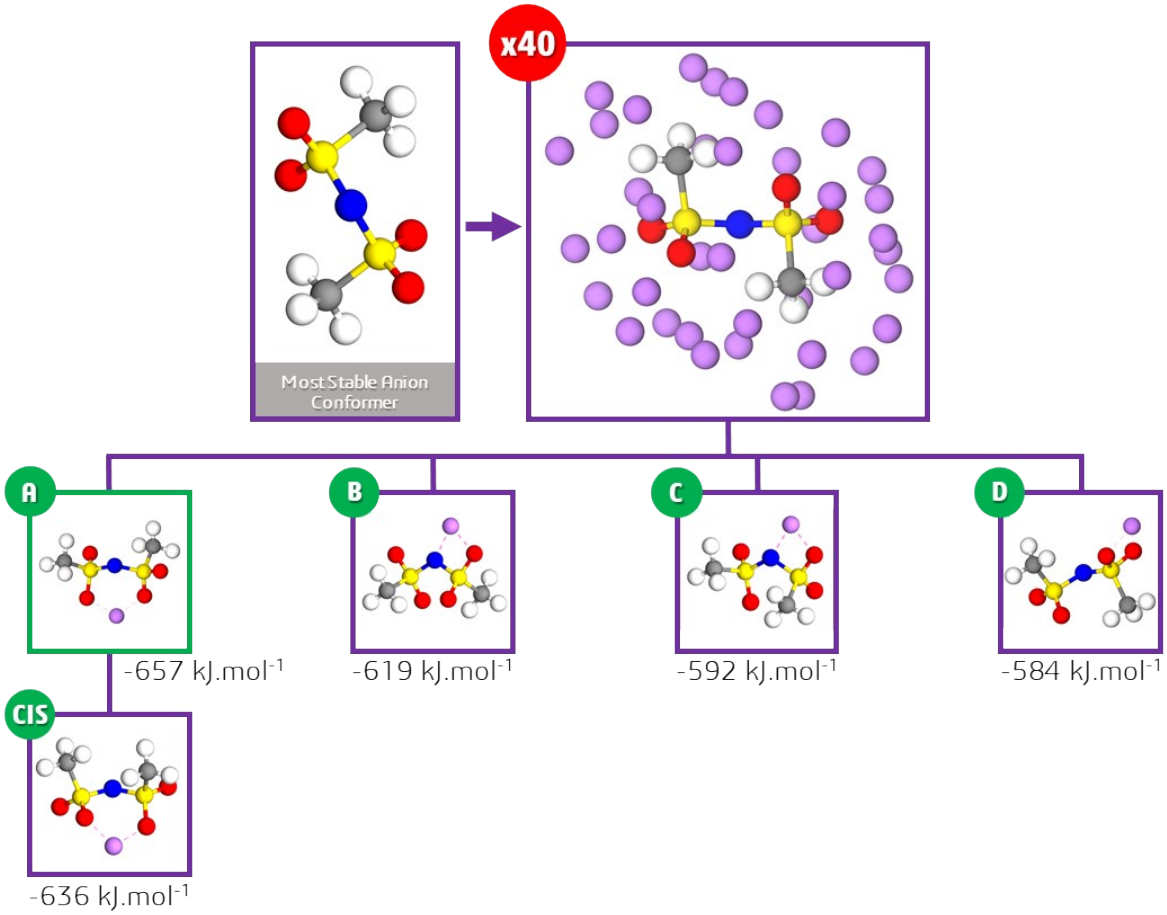


**Figure S4** – Conformer scan and lithiation site screening of $S_1$ ($MSI^-$), depicting the 5 calculated unique adsorption sites and binding energies. The most stable site is outlined in green.

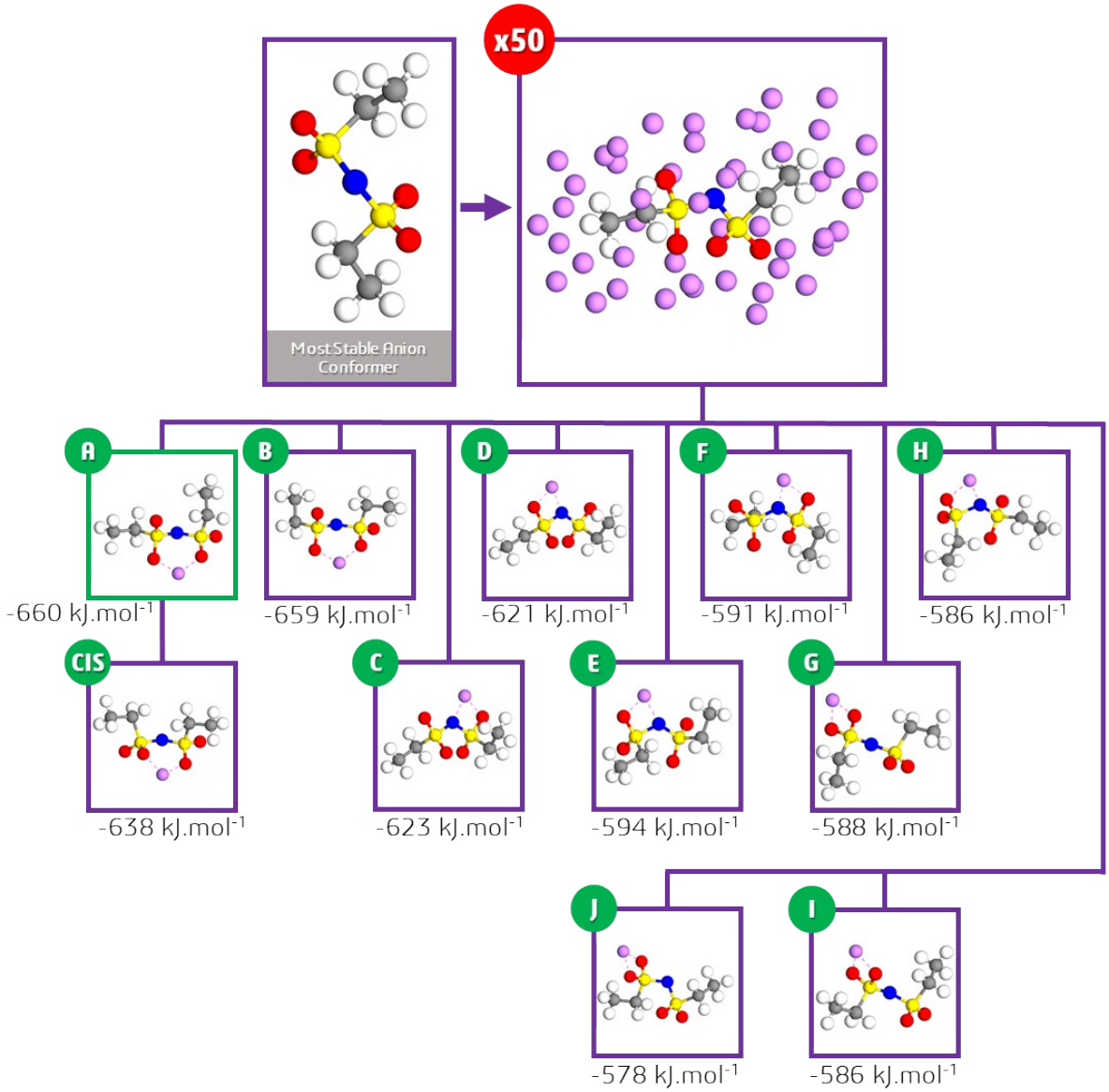


**Figure S5** – Conformer scan and lithiation site screening of $S_2$ ($ESI^-$), depicting the 11 calculated unique adsorption sites and binding energies. The most stable site is outlined in green.

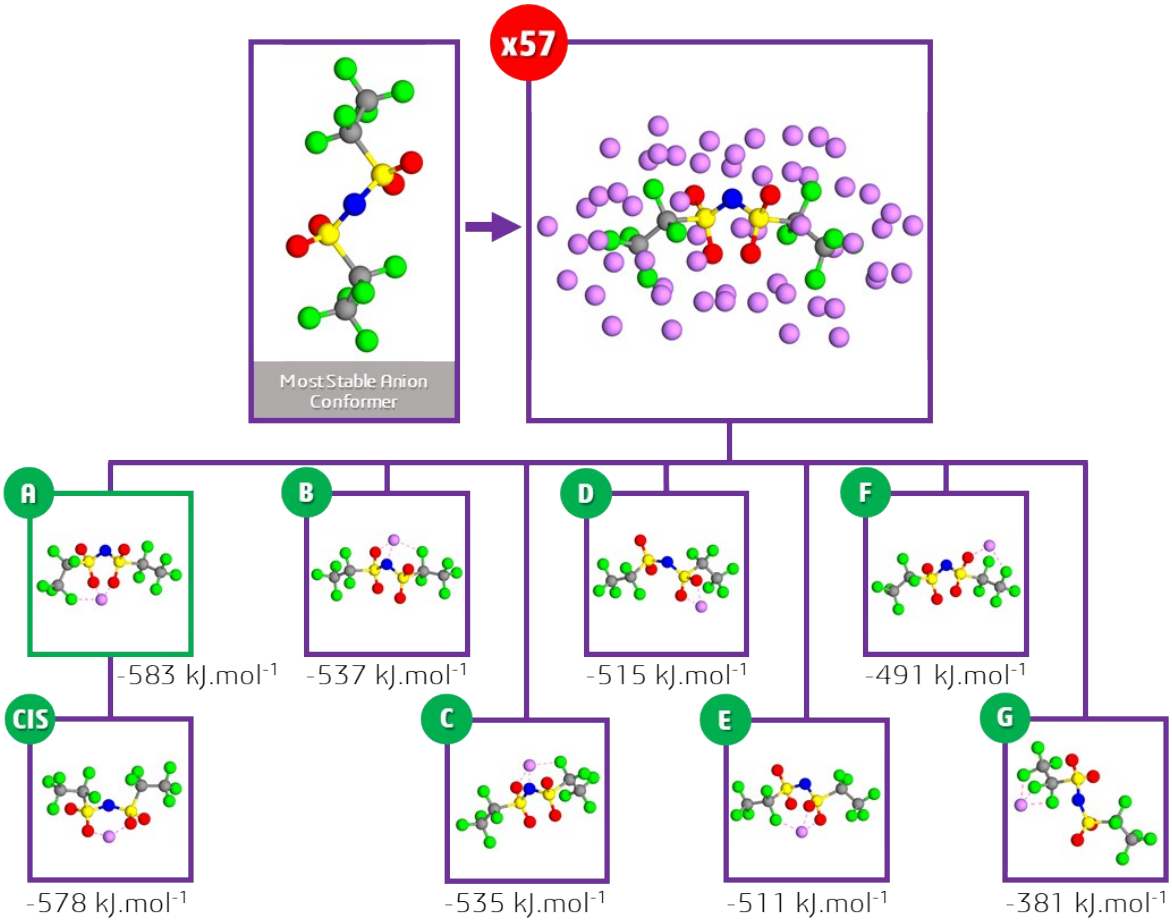


**Figure S6** – Conformer scan and lithiation site screening of $S_3$ ($BETI^-$), depicting the 8 calculated unique adsorption sites and binding energies. The most stable site is outlined in green.

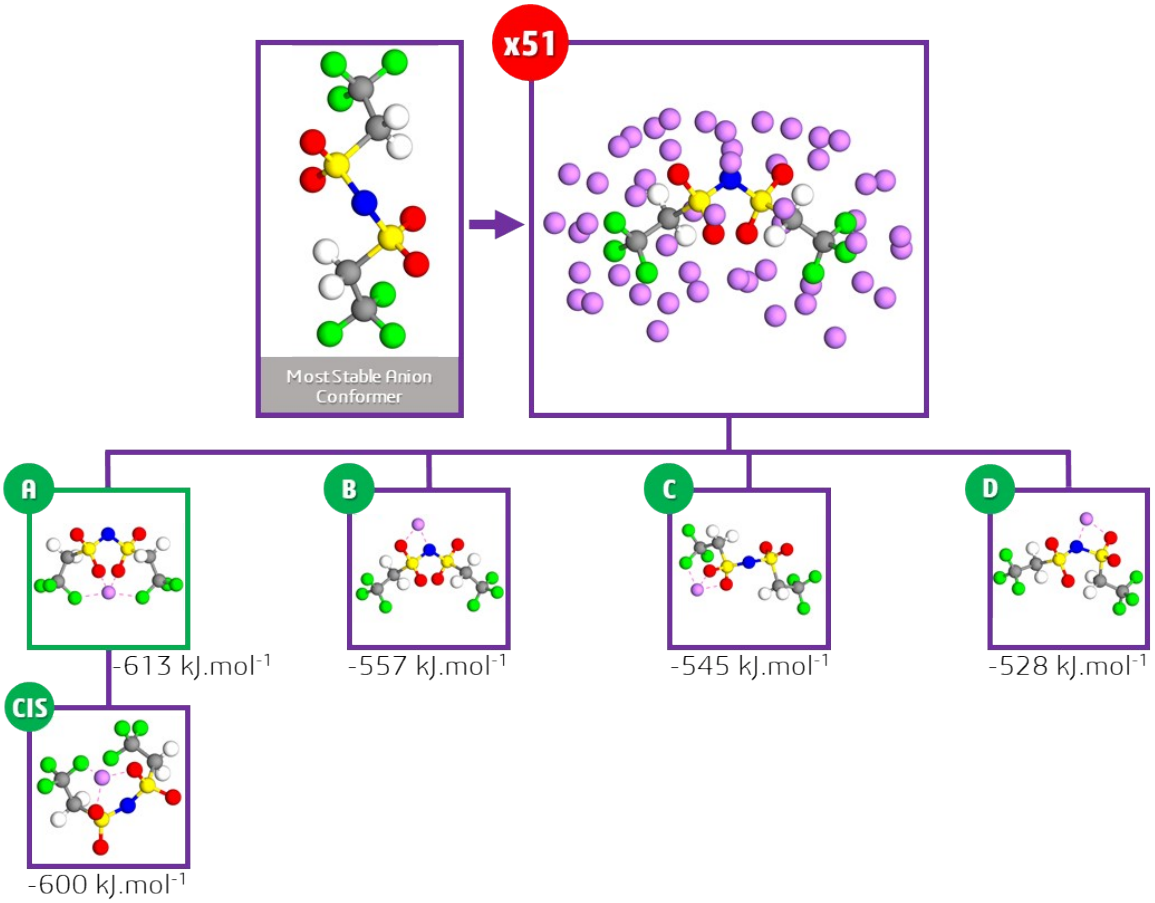


**Figure S7** – Conformer scan and lithiation site screening of $S_4$ ($TFESI^-$), depicting the 5 calculated unique adsorption sites and binding energies. The most stable site is highlighted in green.

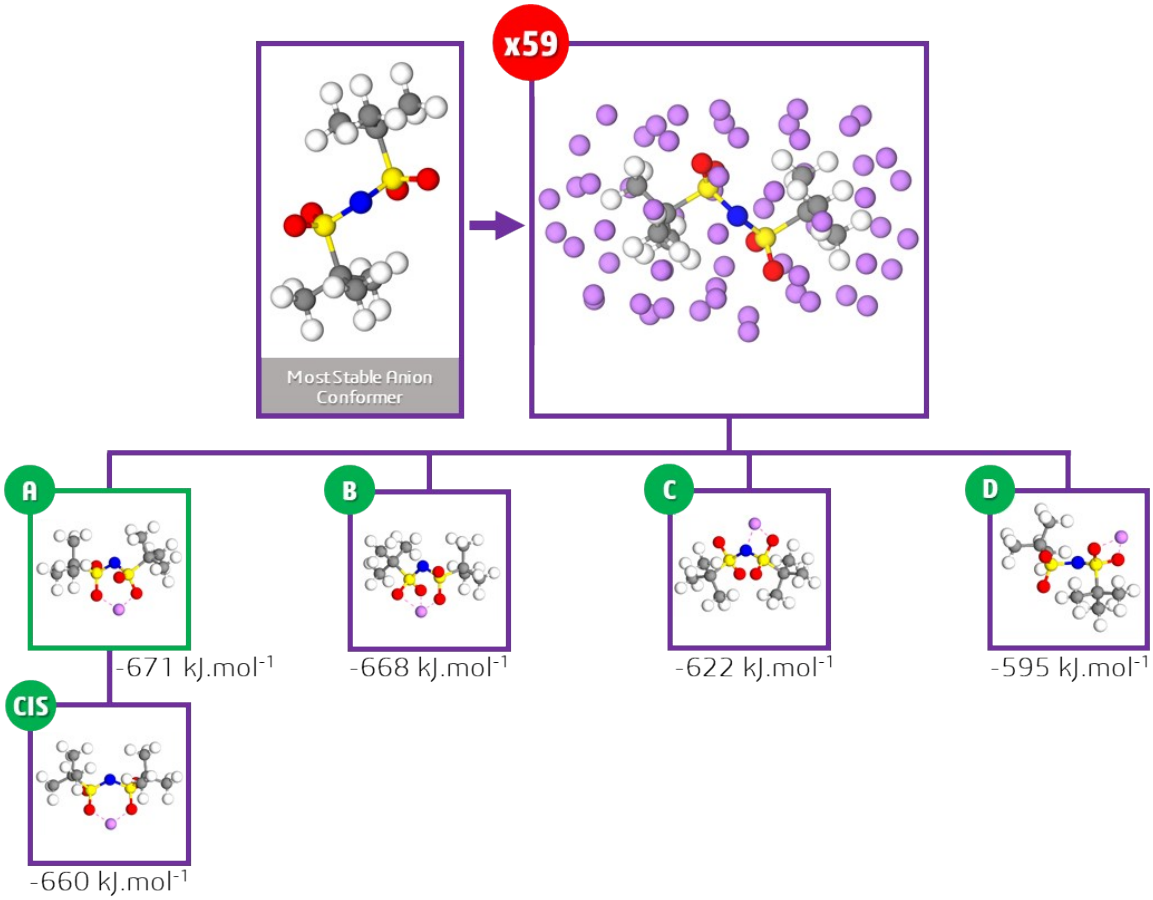


**Figure S8** – Conformer scan and lithiation site screening of $S_5$ ($TbSI^-$), depicting the 5 calculated unique adsorption sites and binding energies. The most stable site is highlighted in green.

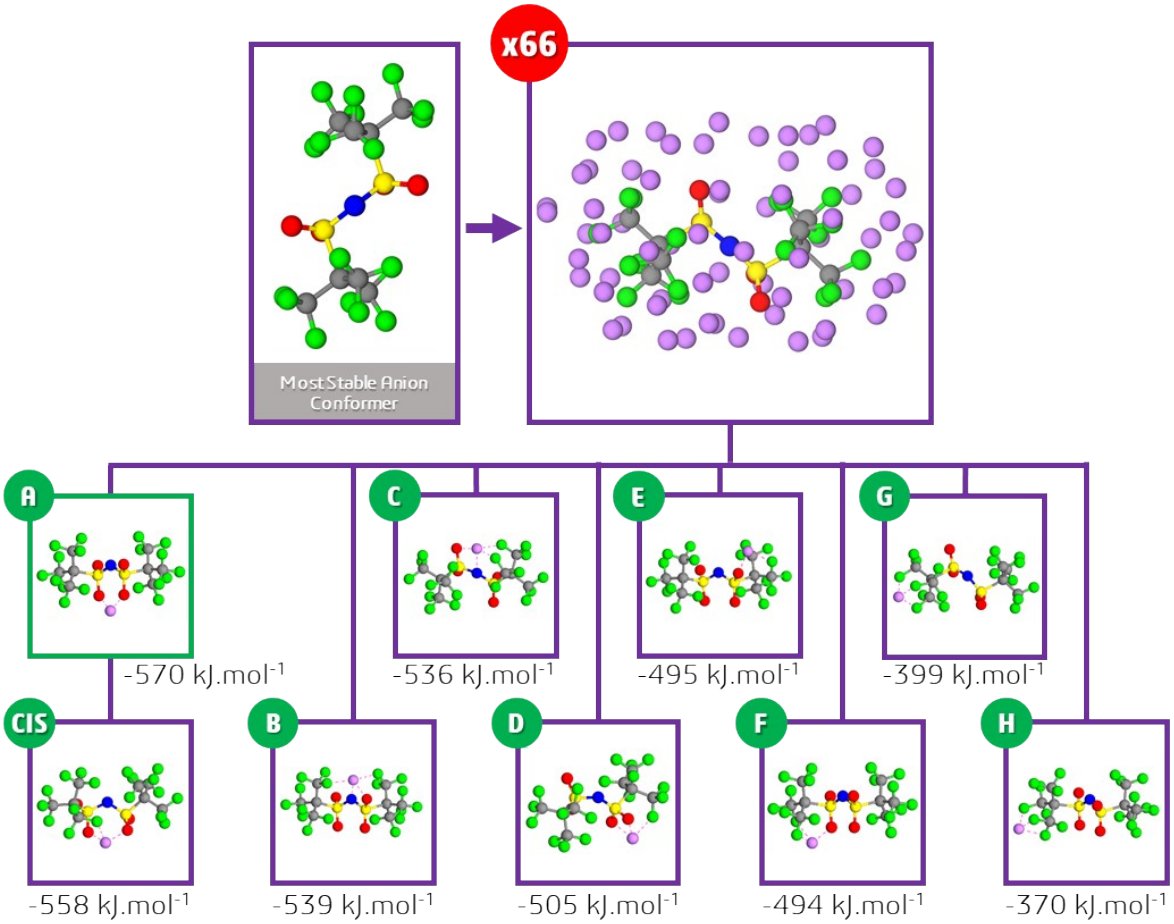


**Figure S9** – Conformer scan and lithiation site screening of $S_6$ ($NFSI^-$), depicting the 9 calculated unique adsorption sites and binding energies. The most stable site is outlined in green.

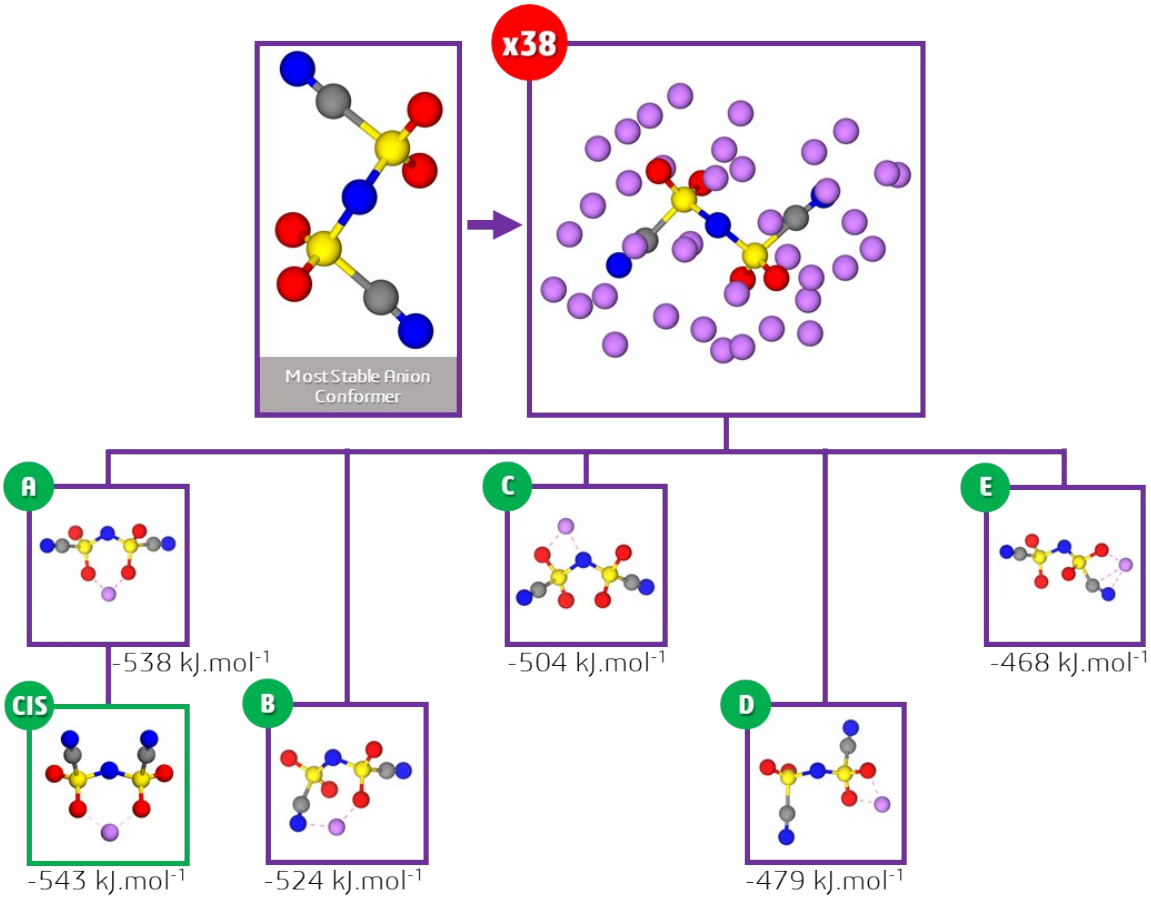


**Figure S10** – Conformer scan and lithiation site screening of $S_7$ ($CSI^-$), depicting the 6 calculated unique adsorption sites and binding energies. The most stable site is outlined in green.

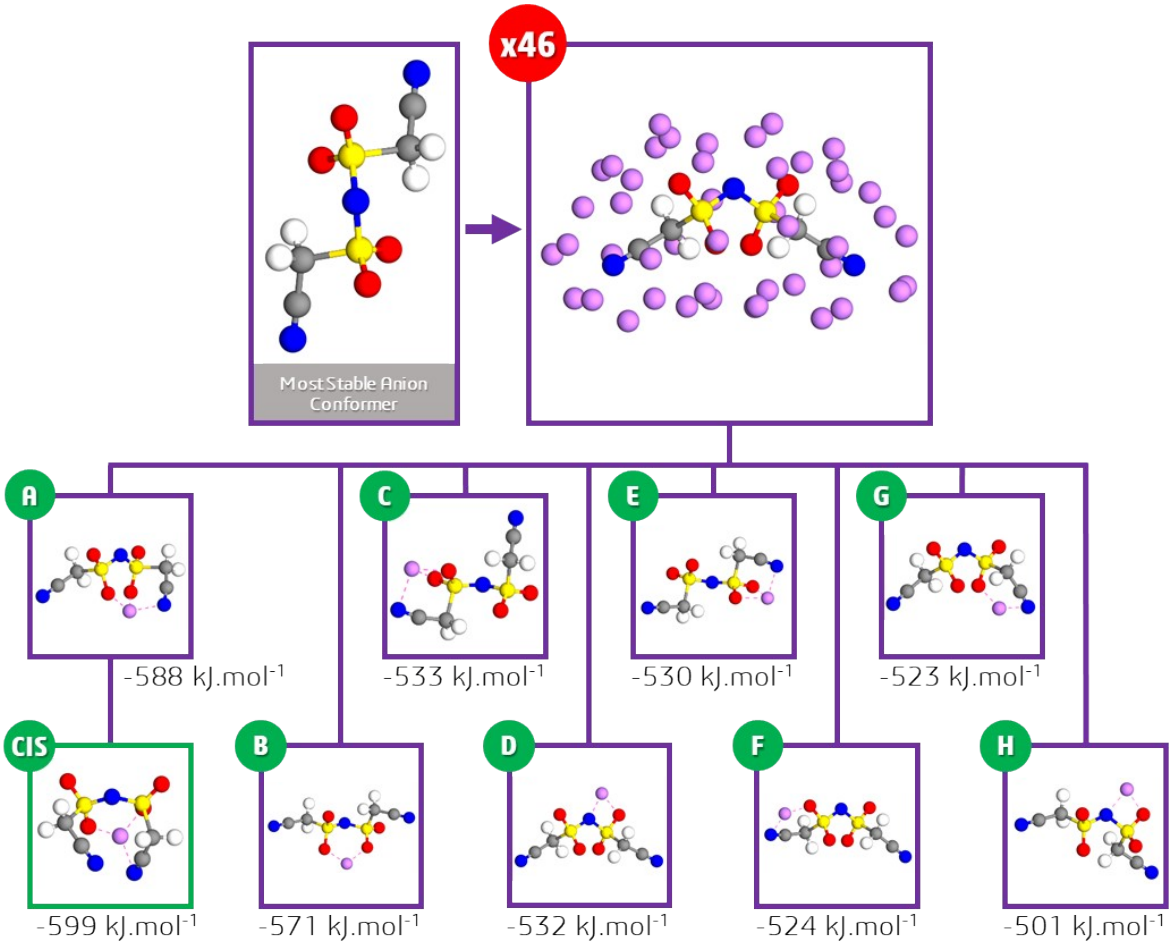


**Figure S11** – Conformer scan and lithiation site screening of $S_8$ ($CmSI^-$), depicting the 9 calculated unique adsorption sites and binding energies. The most stable site is outlined in green.

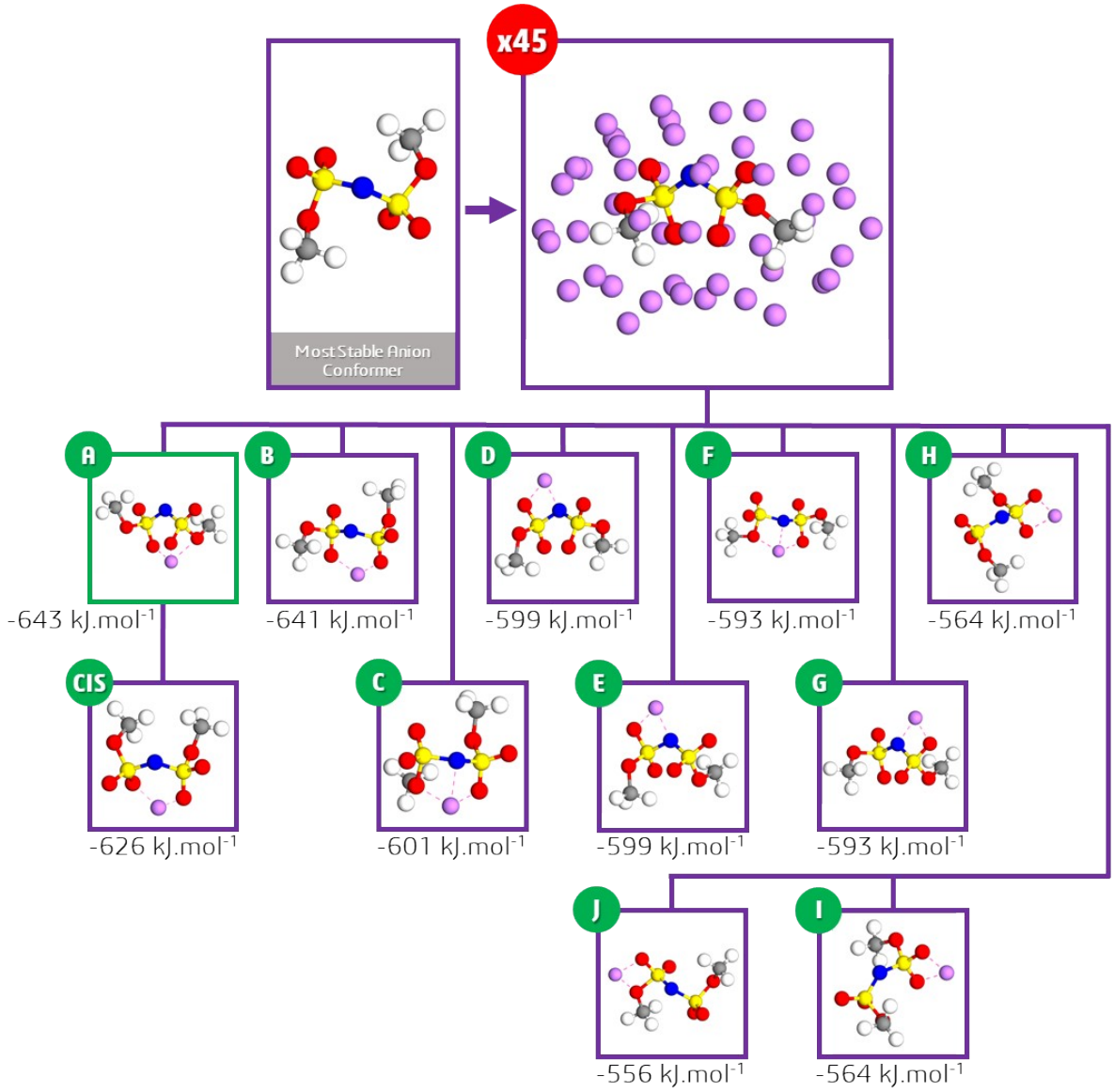


**Figure S12** – Conformer scan and lithiation site screening of $S_9$ ($MOSI^-$), depicting the 11 calculated unique adsorption sites and binding energies. The most stable site is outlined in green.

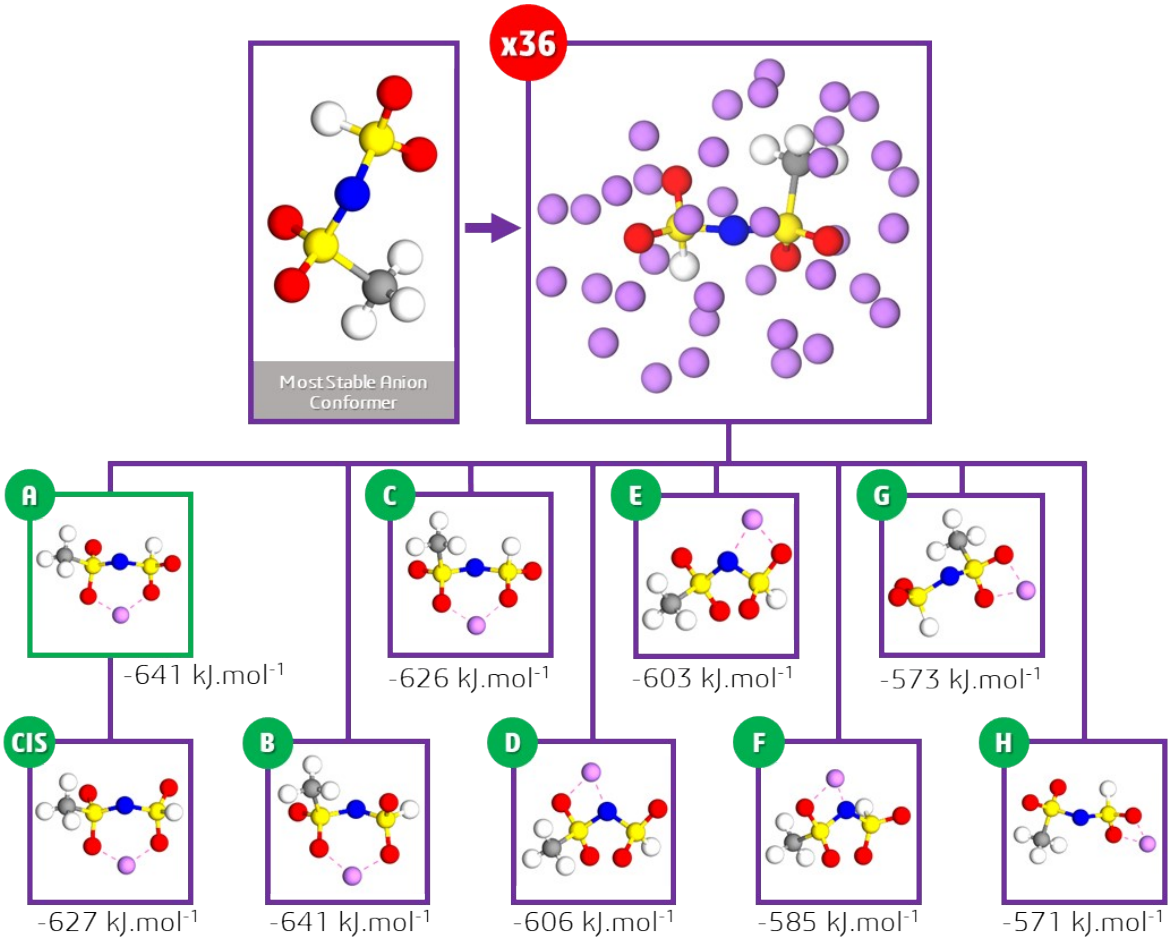


**Figure S13** – Conformer scan and lithiation site screening of $A_1$ ($HMSI^-$), depicting the 9 calculated unique adsorption sites and binding energies. The most stable site is outlined in green.

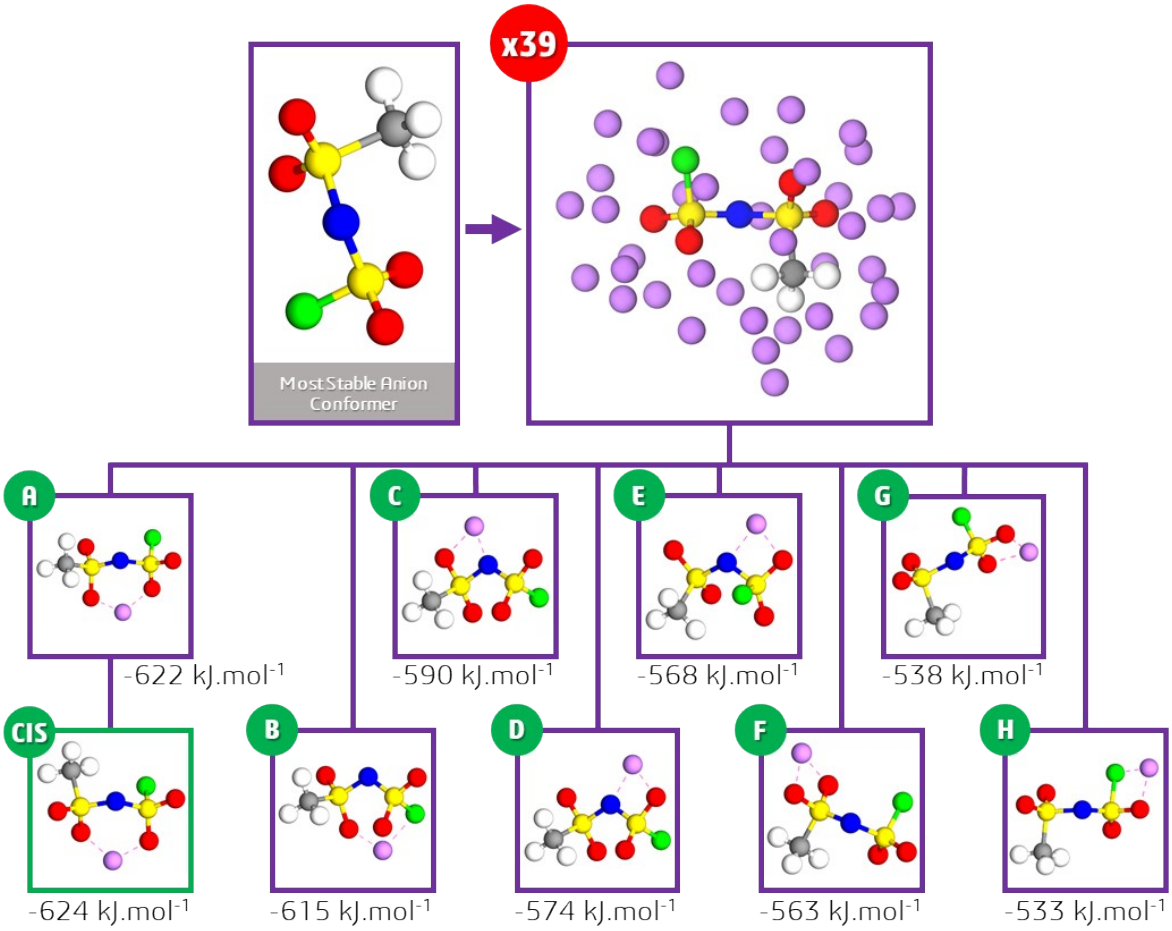


**Figure S14** – Conformer scan and lithiation site screening of $A_2$ ($FMSI^-$), depicting the 9 calculated unique adsorption sites and binding energies. The most stable site is highlighted in green.

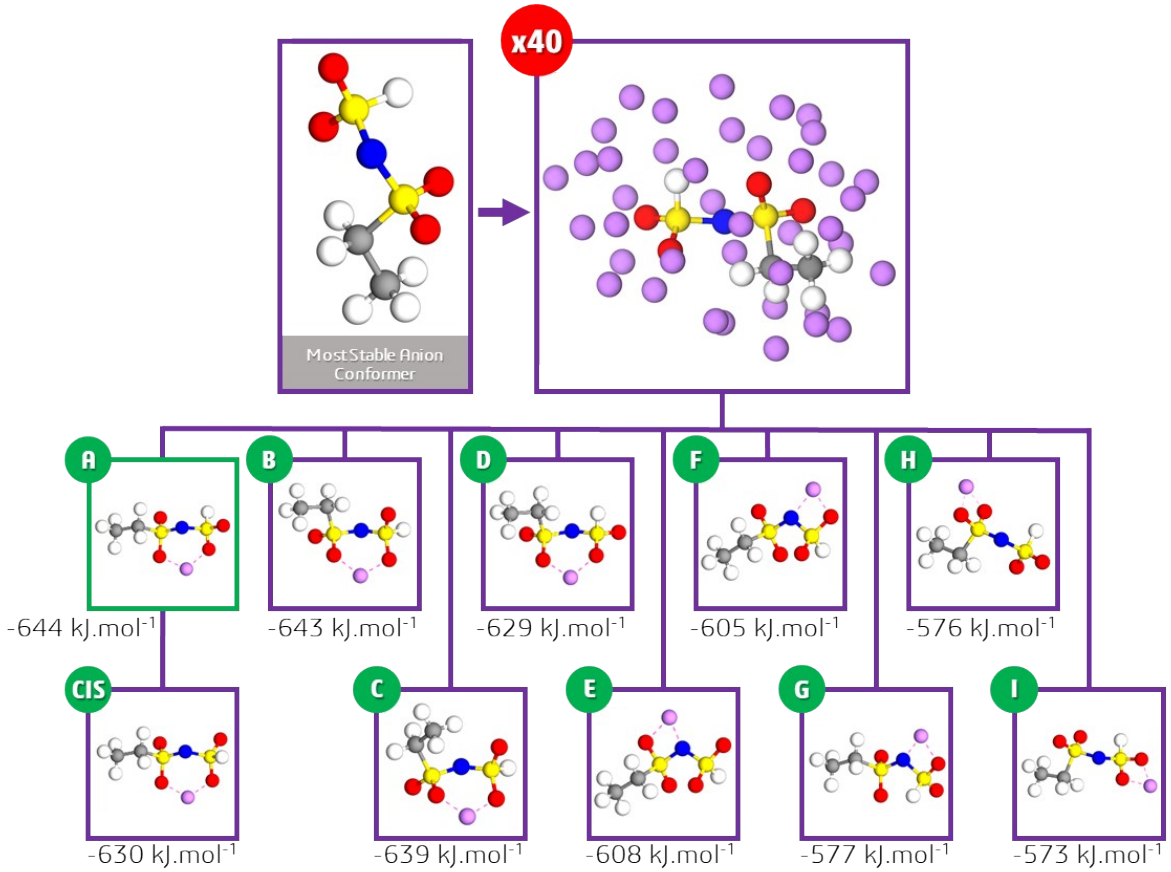


**Figure S15** – Conformer scan and lithiation site screening of $A_3$ ($HESI^-$), depicting the 10 calculated unique adsorption sites and binding energies. The most stable site is outlined in green.

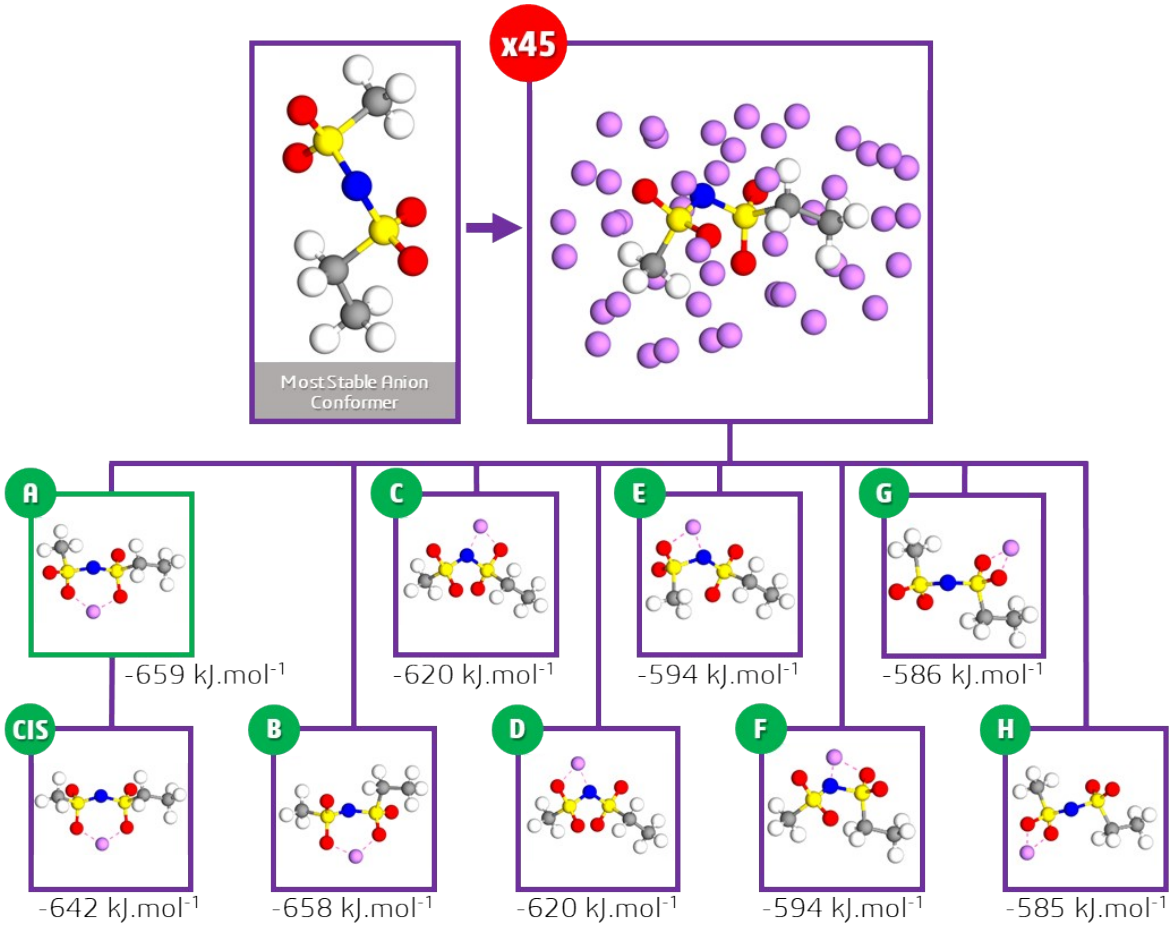


**Figure S16** – Conformer scan and lithiation site screening of A4 (MESI-), depicting the 9 calculated unique adsorption sites and binding energies. The most stable site is outlined in green.

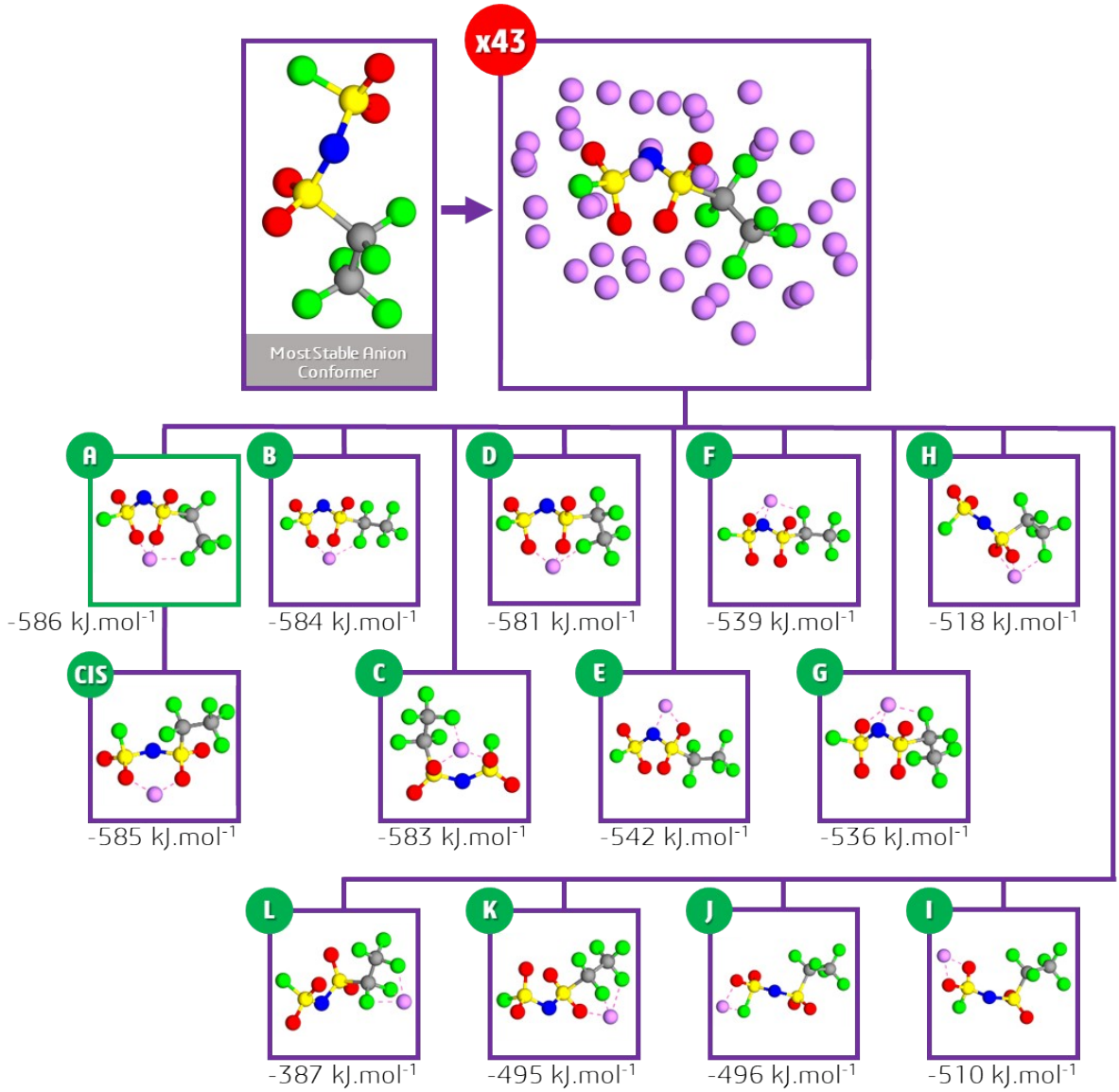


**Figure S17** – Conformer scan and lithiation site screening of $A_5$ ($FPFESI^-$), depicting the 13 calculated unique adsorption sites and binding energies. The most stable site is outlined in green.

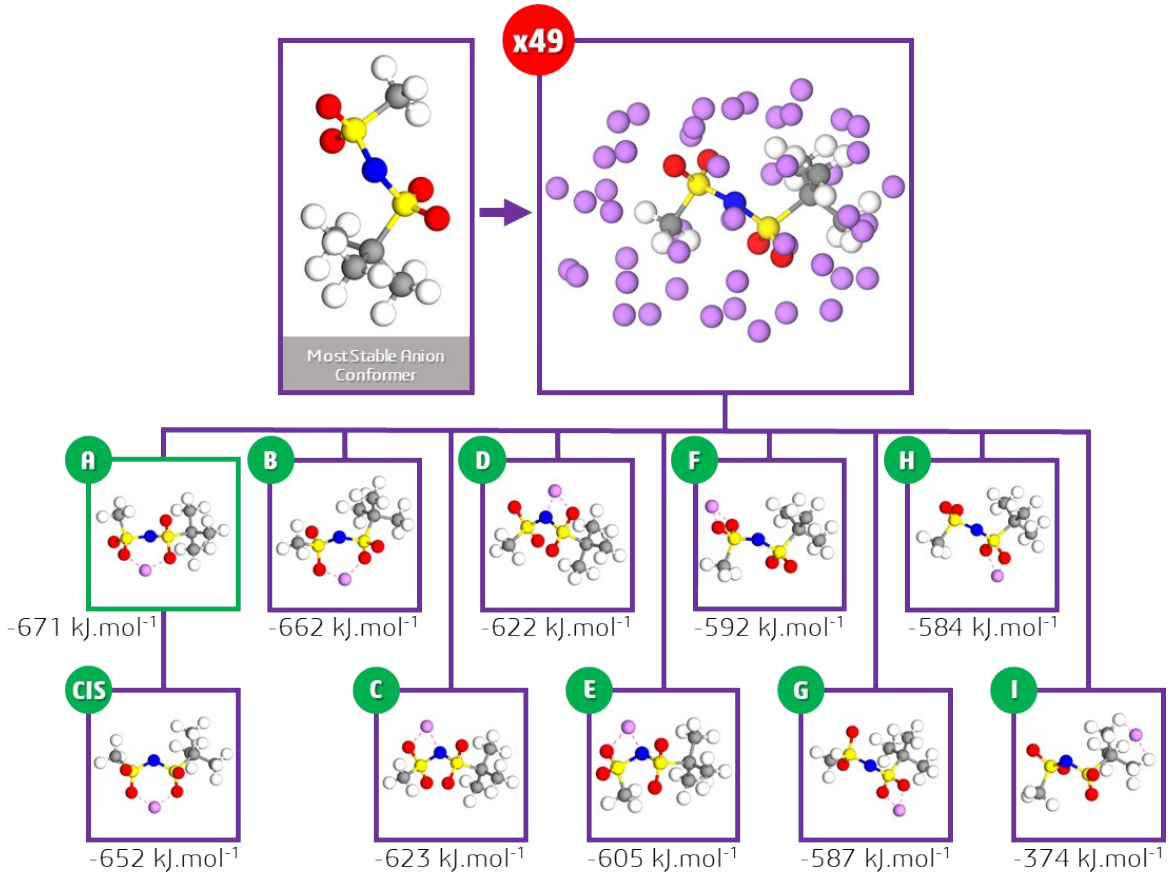


**Figure S18** – Conformer scan and lithiation site screening of $A_6$ ($MTbSI^-$), depicting the 10 calculated unique adsorption sites and binding energies. The most stable site is outlined in green.

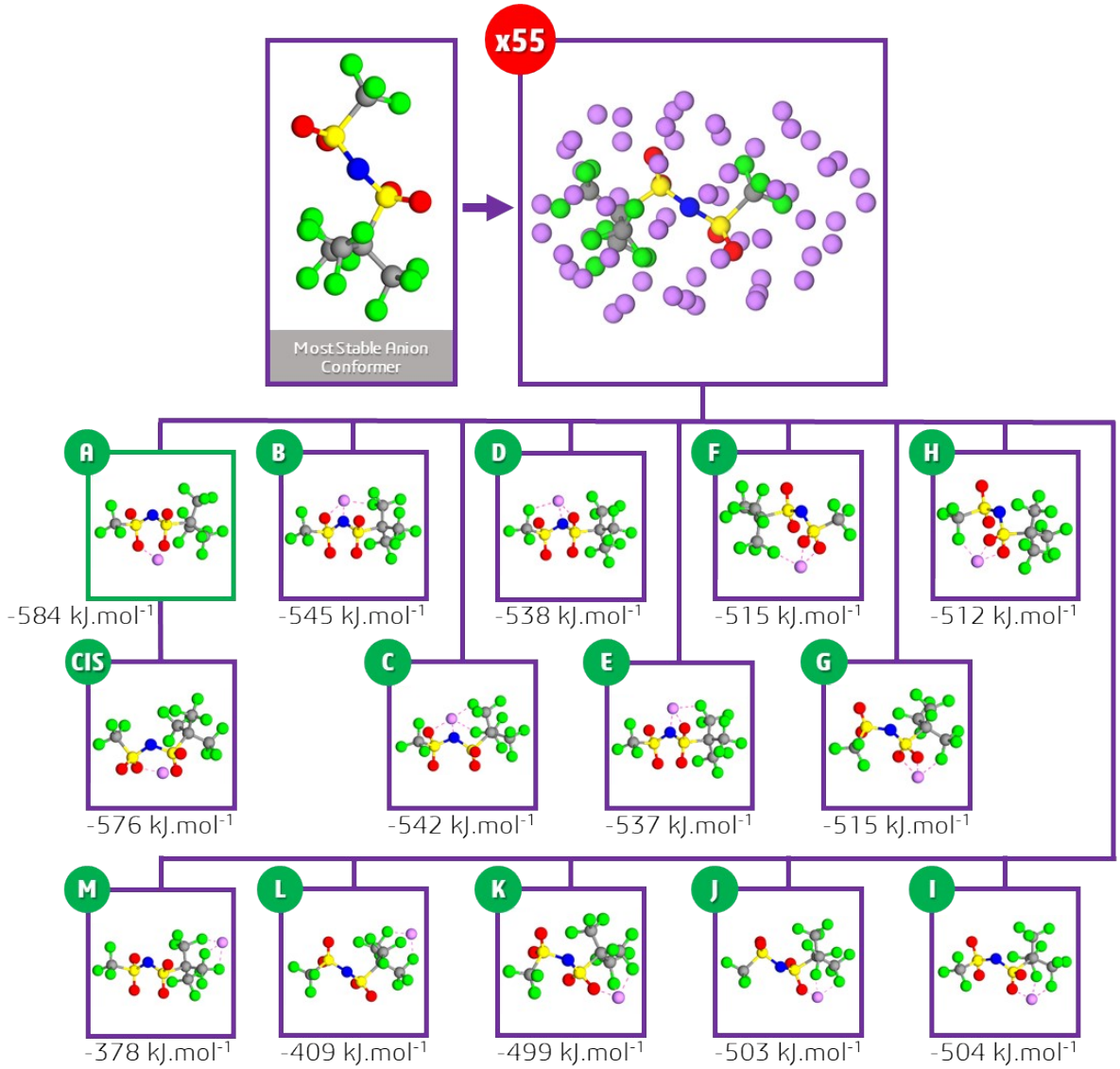


**Figure S19** – Conformer scan and lithiation site screening of $A_7$ ($TFNFSI^-$), depicting the 14 calculated unique adsorption sites and binding energies. The most stable site is outlined in green.

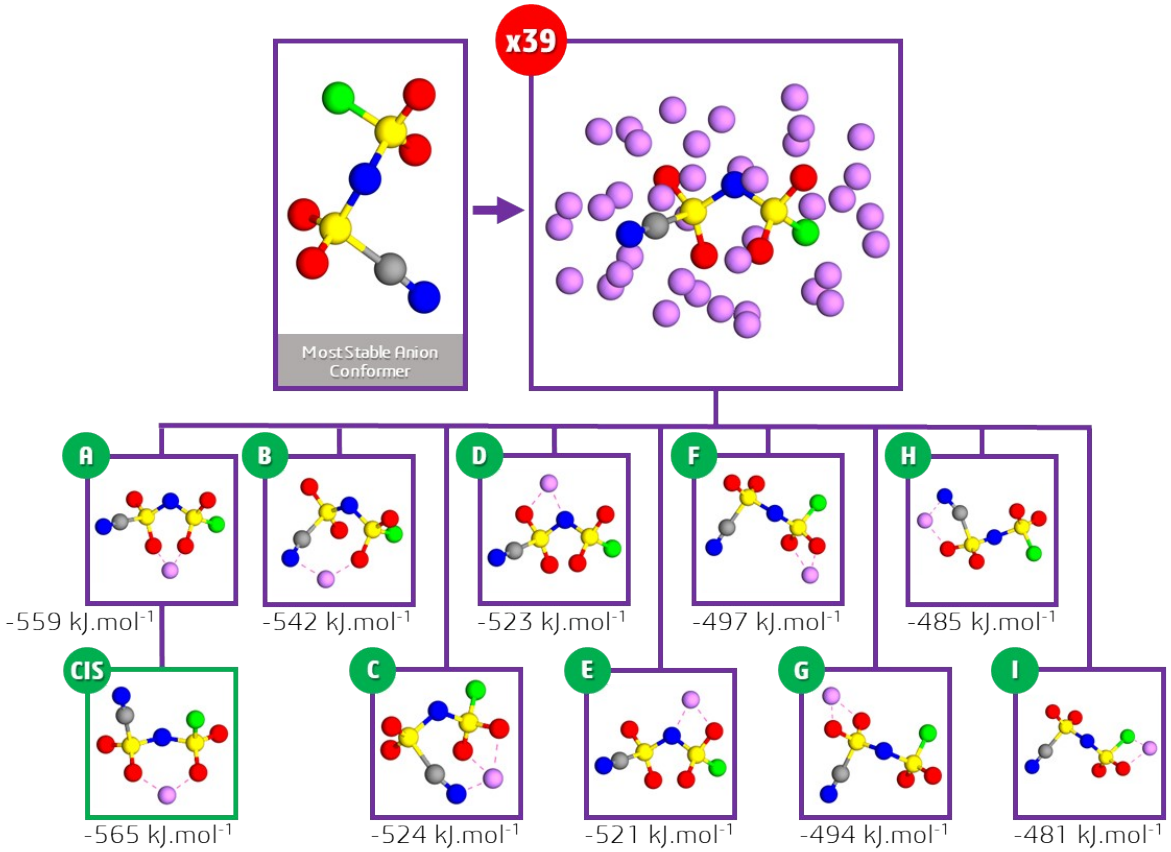


**Figure S20** – Conformer scan and lithiation site screening of A8 (FCSI-), depicting the 10 calculated unique adsorption sites and binding energies. The most stable site is outlined in green.

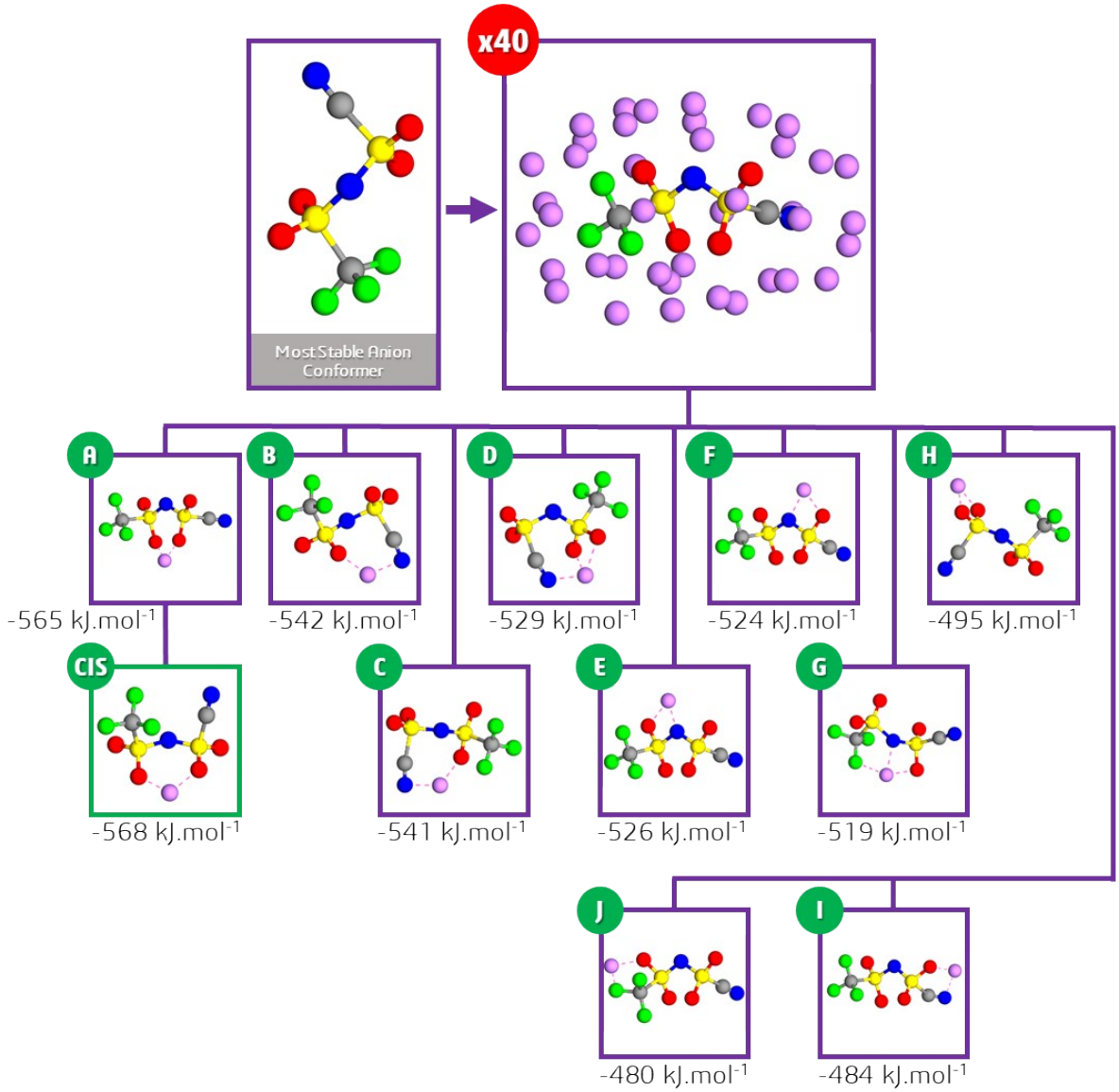


**Figure S21** – Conformer scan and lithiation site screening of $A_9$ ($TFCSI^-$), depicting the 11 calculated unique adsorption sites and binding energies. The most stable site is outlined in green.

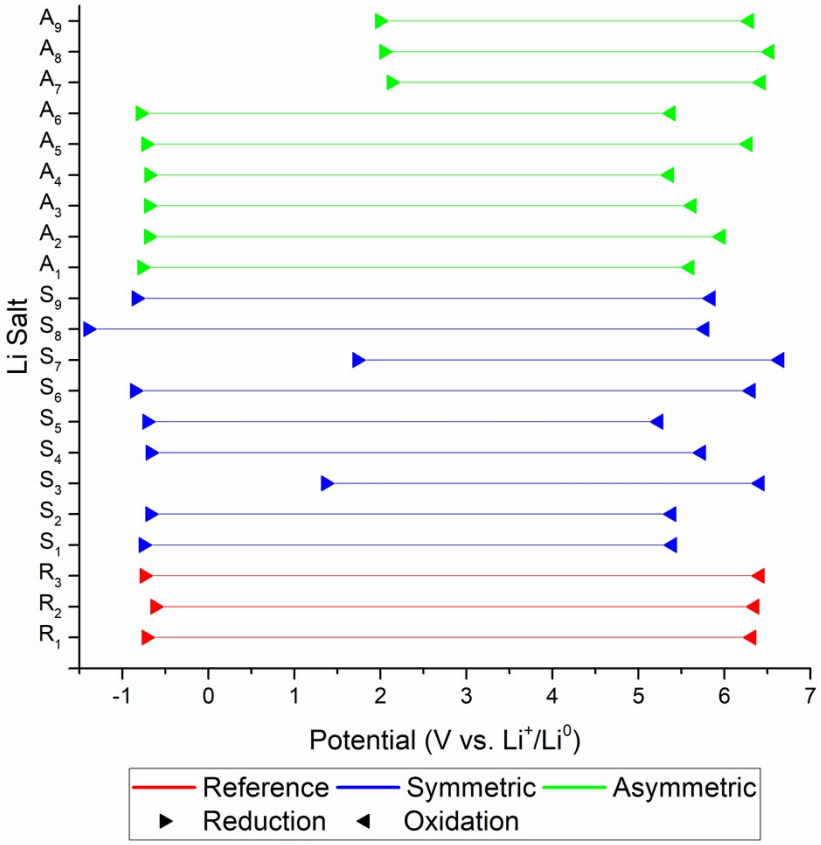


**Figure S22** –Calculated electrochemical windows for the reference, symmetric and asymmetric salts.